Original Article

# Prognostic evaluation of a multi-target magnetic bead-enriched circulating tumor cell-enriched identification system for colorectal cancer

**Yanfu Wang[1#], Lu Xia[2#], Mei Wu[2], Chunjin Huang[1]**

[1]General Surgery Department, Huadong Hospital Affiliated to Fudan University, Shanghai, China; [2]Day Surgery Unit, Huadong Hospital Affiliated to Fudan University, Shanghai, China

*Contributions:* (I) Conception and design: Y Wang, L Xia; (II) Administrative support: C Huang; (III) Provision of study materials or patients: C Huang; (IV) Collection and assembly of data: M Wu; (V) Data analysis and interpretation: M Wu; (VI) Manuscript writing: All authors; (VII) Final approval of manuscript: All authors.

[#]These authors contributed equally to this work.

*Correspondence to:* Chunjin Huang, MM. General Surgery Department, Huadong Hospital Affiliated to Fudan University, 221 Yanan West Road, Shanghai 200040, China. Email: bigtigerhuang@126.com.

**Background:** Colorectal cancer (CRC) is the third most prevalent cancer in the world. Traditional tissue biopsy cannot provide dynamic monitoring of patients' tumors or reflect the characteristics of tumors in real time because the sampling process is invasive and accompanied by risks. Circulating tumor cells (CTCs) are considered a major cause of tumor metastasis, and investigating CTCs helps to understand the biology and vulnerability of malignant tumors during hematogenous metastasis.

**Methods:** We sequentially used epithelial cell adhesion molecule (EpCAM)-coated immunoliposomal magnetic beads (Ep-IMBs) and vimentin-coated immunoliposomal magnetic beads (Vi-IMBs) to capture and characterize CTCs from 110 CRC patients. We further constructed a Cox risk regression model, optimized the model composition using backward stepwise regression, and finally applied nomograms to show the effect of each variable on survival risk.

**Results:** The specificity of the CTCs enrichment and identification system was 100% and the sensitivity was 79.0%. Multivariate analysis indicated total CTC number was an important predictor for bad survival, whereas American Joint Committee on Cancer (AJCC) stage, lymph node metastasis, and carcinoembryonic antigen (CEA) level were associated with prognosis, and the risk of mortality was associated with the AJCC stage of the CRC.

**Conclusions:** The CTC enrichment and identification system constructed in this research demonstrated superior accuracy. In addition, CTCs can be used as an important predictor for prognosis of patients with CRC, and the combination of other clinical predictive factors can help clinicians to better design individualized treatment regimens, which is of great clinical application value.

**Keywords:** Colorectal cancer (CRC); prognostic; circulating tumor cells (CTCs); cancer risk factor

Submitted Aug 31, 2023. Accepted for publication Jan 16, 2024. Published online Feb 28 2024.
doi: 10.21037/jgo-23-735
**View this article at:** https://dx.doi.org/10.21037/jgo-23-735

## Introduction

Colorectal cancer (CRC) is the third most prevalent cancer in the world. It is estimated that almost two million patients will be diagnosed with CRC each year, of which 950,000 will die. The new cases of CRC have been escalating every year for the past decade, and patient survival rates are increasing (1). The number of deaths from CRC is expected to exceed 1 million per year globally by 2030 (2). The diagnosis of CRC is currently performed mainly by pathological biopsy (3). Previous studies have identified a number of protein biomarkers which are highly associated with CRC using immunohistochemistry. Research has shown that in addition to carcinoembryonic antigen (CEA), carbohydrate antigen 19-9 (CA19-9), epithelial cell adhesion molecule (EpCAM), and caudal-type homeobox 2 (CDX2) were highly specific for intestinal epithelial cells, and glycoprotein A33 (GPA33) was usually expressed on well-differentiated CRC (4-6). If metastasis is suspected, it is confirmed by medical imaging technology, which can be enhanced by biochemical tests such as CEA (7). However, traditional tissue biopsy cannot provide dynamic monitoring of patients and cannot reflect the characteristics of tumors in real time because the sampling process is invasive and accompanied by risks, so there is an urgent clinical need for safer and more efficient methods to monitor tumor development and treatment response. This can serve as an effective supplement to traditional biopsy methods.

Tumor cells undergoing epithelial-mesenchymal transition (EMT), enhanced migration, and vascular invasion breakaway from the primary lesion and enter the circulation, and eventually become the seeds of distant metastases. CTCs are considered a major cause of tumor metastasis, and investigating CTCs can help to elucidate the biology and vulnerability of malignant tumors during hematogenous metastasis (8). Altered biochemical functions directed by CTCs undergoing EMT markedly enhance CTC metastatic invasion and treatment resistance, in addition to the identification of CTC morphology and downstream analysis with the help of fluorescence microscopy, all of which are unique advantages of CTCs in clinical applications (9). The most common method of CTC enrichment involves using the mechanism of antigen-antibody-specific binding, relying on markers specifically expressed on the CTC surface to enrich tumor cells and immobilize them on a magnetic frame, and many kinds of markers are currently identified on the CTC surface as well (10). This platform specifically captures $EpCAM^+$ tumor cells from the peripheral blood (PB) of patients through ferrofluidic nanoparticles. CellSearch® has demonstrated through numerous clinical trials that CTCs detected by this method have a close relationship with patient prognosis, and some studies have shown that tumor cells enriched by CellSearch® are of great value in clinical research (11-15). However, CellSearch® based on an EpCAM-based enrichment strategy has some limitations. Firstly, this method may overlook CTCs that poorly express or have a lack of epithelial surface markers (16). Secondly, CellSearch® is also unable to interstitially identify tumors that express little or no EpCAM of mesenchymal origin, as well as epithelial-derived CTCs that are partially in EMT; several published reports have highlighted this issue (11,17-21), which severely limits the clinical application of CellSearch®. In this study, we constructed a novel multiplexed magnetic bead enrichment platform in which we used EpCAM-coated immunoliposomal magnetic beads (Ep-IMBs) and vimentin-coated immunoliposomal magnetic beads (Vi-IMBs) sequentially to capture CTCs. This approach significantly improved the sensitivity of CTCs compared to the EpCAM-based strategy, thus enhancing the diagnostic efficacy of the system. We analyzed the difference in the amount of CTCs in PB between healthy volunteers and patients with CRC and attempted to analyze the correlation between CTCs and clinical outcomes in patients with CRC. We present this article in accordance with the TRIPOD reporting checklist (available at https://jgo.amegroups.com/article/view/10.21037/jgo-23-735/rc).

### Highlight box

**Key findings**

- The multi-target magnetic bead-constructed circulating tumor cells (CTCs) capture method has excellent diagnostic efficacy and prognostic value for patients with colorectal cancer (CRC).

**What is known and what is new?**

- CTCs can be used for early diagnosis of malignant tumors and assessment of prognosis, but in CRC, relevant studies are still limited.
- In this study, the role of CTCs in the early diagnosis of CRC, as well as in the assessment of patient prognosis, was validated by following up with patients' clinical data.

**What is the implication, and what should change now?**

- The evidence for the clinical use of CTCs in CRC has been further refined, and therefore CTCs should be used in the daily management of CRC patients and treatment strategies should be promptly adjusted according to the results of CTCs.

 

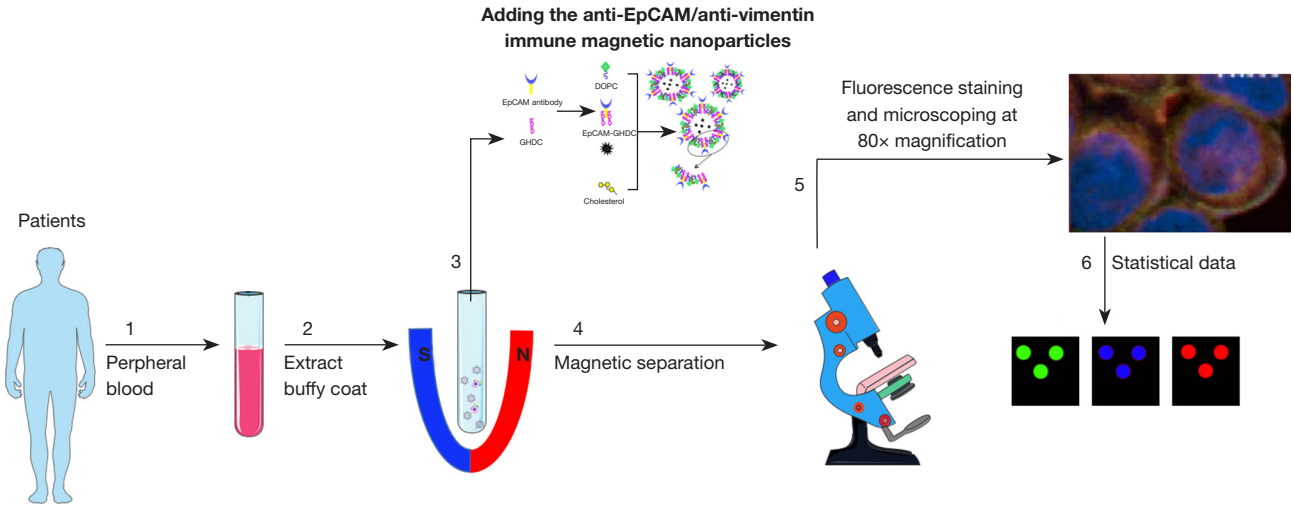


**Figure 1** Schematic diagram of multi-target immunomagnetic bead CTC assay. EpCAM, epithelial cell adhesion molecule; GHDC, dimethyl octadecyl epoxypropyl ammonium chloride; DOPC, 1,2-dioleylphosphatidylcholine; CTC, circulating tumor cell.

## Methods

### *Patients and CTC sample*

This study included 110 patients with CRC treated in the General Surgery Department of Huadong Hospital Affiliated to Fudan University between 1 May 2016 and 31 December 2019. Blood samples were obtained at 1 day prior to surgery, then were sent to Huzhou Lieyuan Medical Testing Co., Ltd. for CTC analysis. The patients' tumor site, American Joint Committee on Cancer (AJCC) stage, CEA level, and other data were also collected. The study was conducted in accordance with the Declaration of Helsinki (as revised in 2013) and was approved by the Ethics Committee of the Huadong Hospital Affiliated to Fudan University (No. 20230056). The inclusion criteria were as follows: (I) age 18–90 years; (II) presence of histologically confirmed CRC (AJCC stages I–IV); and (III) written informed consent has been signed from patients before participation. The exclusion criteria were as follows: (I) unresectable primary tumor or metastasis; (II) undergoing any treatment (including chemotherapy, radiotherapy, and targeted therapy) prior to surgery; and (III) concurrent presence of other malignant tumors. Patients were followed up in the first month post therapy, thereafter, a review was performed every 3 months. The observational endpoint of this study was overall survival (OS), with a median follow-up time of 2 years. To investigate the detection rate of CTC in CRC patients and healthy people, we recruited 25 healthy volunteers at the same time and collected 7.5 mL blood samples as negative controls. The schematic diagram of multi-target immunomagnetic bead CTC assay is shown in *Figure 1*.

### *Preparation of liposomal magnetic beads*

As previously reported (22), we adjusted the dose of dimethyl octadecyl epoxypropyl ammonium chloride (GHDC) to obtain immunoliposomal magnetic beads (IMBs) with gradient concentration of antibody. Water-soluble antibodies showed good solubility in organic solvents after the addition of hydrophobic side chains of long-chain alkyl groups. Ep-IMB was prepared from EpCAM, cholesterol (Chol), and 1,2-dioleylphosphatidylcholine (DOPC) by reverse evaporation method. The weight ratio of DOPC to Chol was fixed at 3:2, and the weight ratio of amphiphilic antibody (AA) to Chol could be between 0 and 2.5. Also, the EpCAM antibody content in Ep-IMB could be adjusted, and the optimal content of EpCAM antibody was determined by subsequent experiments. Vi-IMB was also prepared by a similar method.

### *Cytotoxicity evaluation of immune magnetic beads*

Human CRC cells SW480, SW620, LOVO, HT-29 were prepared. A 500 μL quantity of trypsin was added and the cells were incubated for 5 minutes. A blood cell counter was used to inhale the cell suspension and adjust the concentration of cell suspension, then 1,000 cells/well were added in a 96-well plate. Next, 250 μL/well of Roswell Park

 

Memorial Institute (RPMI) 1640 medium was added and in order to evaluate the growth inhibitory effect of gradient concentration of IMB on tumor cells, we added gradient concentrations of IMB to inhibit the growth of tumor cells. The cells were then incubated under the conditions of 5% $CO_2$, 37 ℃, and then 10 μL 3-(4,5-dimethylthiazol-2-yl)-2,5-diphenyltetrazolium bromide (MTT) solution (5 mg/mL) was added to each well and further incubated for 4–6 hours after removing the culture fluid in the wells. We added 150 μL dimethyl sulfoxide (DMSO), and then used an enzyme marker to detect the wavelength of each well and an enzymometer to detect the absorbance value of each well at a wavelength of 450 nm.

### *IMB capture tumor cell specificity assay*

In order to comprehensively investigate the effects of various magnetic bead mating protocols on the capture efficiency of tumor cells, we set up five experimental groups, namely Ep-IMB group, Vi-IMB group, Ep/Vi-IMB group, Ep-IMB + Vi-IMB group, and Vi-IMB + Ep-IMB group. LOVO cells were removed for cell counting under an inverted fluorescence microscope. We added 100 μL of cell suspension to 7.5 mL of phosphate buffer solution (PBS), and 10, 15, 20, and 30 μL of Ep-IMB or Vi-IMB was added to the Ep-IMB group and Vi-IMB group, respectively. In the EP-/Vi-IMB group, 10, 15, 20, and 30 μL of equal volumes of Ep-IMB and Vi-IMB mixtures were added, respectively. In the Ep-IMB + Vi-IMB group, equal volumes of EP-IMB and Vi-IMB were added sequentially to enrich tumor cells. In the Vi-IMB + Ep-IMB group, the order of addition of the two types of magnetic beads was switched. In the experiment of optimizing the proportion of IMBs to antibody, 10, 50, 100, 200, and 1,000 LOVO cells were captured with 10 μL of IMB encapsulated with a gradient concentration of antibody, and the optimal bead-to-antibody ratio was determined according to the capture effect. Then, in order to comprehensively examine the sensitivity and specificity of this capture protocol, we chose SW480, SW620, LOVO, and HT-29 cells, and a gradient number of cells were spiked in 3 mL of PBS to examine the sensitivity of the protocol; PBS was then substituted with blood from healthy volunteers to continue to investigate the specificity of the optimized capture protocol.

### *CTC identification and enumeration*

Ficoll-Paque PLUS (GE Healthcare Pharmacia, Piscataway, NJ, USA) medium was slowly injected into the PB of the patient, centrifuged at 3,000 rpm for 15 minutes, and the PB mononuclear cell (PBMC) layer was separated from the Ficoll-plasma layer interface by density gradient solution, Firstly, 10 μL of Ep-IMB was added to the sample, and the blood was incubated for 15 minutes, then the cells were enriched by the magnetic separation frame, then 10 μL of Vi-IMB was added to the sample, and the enriched cells were obtained by further incubation for 15 minutes, after which 10 μL of 4',6-diamidino-2-phenylindole (DAPI), CK-FITC, and CD45-PE staining solution was sequentially added and incubated for 20 minutes, and the solutions were evenly coated on transparent slides for observation and counting under a three-channel fluorescence microscope.

### *Statistical analysis*

Demographic characteristics and clinicopathological characteristics were summarized statistically. All statistical tests were two-tailed, and all clinical indicators included in the model were screened backward stepwise using the Akaike information criterion (AIC) with estimated risk ratios and 95% confidence intervals (CIs) and plotted in a nomogram.

## Results

### *Preparation of liposomal magnetic beads*

As previously reported, we adjusted the dosage of GHDC to obtain IMB with gradient antibody concentrations. Water-soluble antibodies showed good solubility in organic solvents by the addition of hydrophobic side chains of long-chain alkyl groups. Ep-IMB was produced by reverse evaporation method from EpCAM, Chol, and DOPC. The proportion of DOPC to Chol by weight was anchored at 6:5, and the proportion of AA to Chol by weight was anchored at 2.5:1. Meanwhile, the content of EpCAM antibody in Ep-IMB could be adjusted, and the optimal content of EpCAM antibody was mapped out by subsequent experiments; Vi-IMB was also prepared by a similar method.

### *Cytotoxicity evaluation*

The cytotoxicity assay is shown in *Figure 2A*,*2B*. The average survival rate of CRC cells was higher than 90% with IMB dosage less than 50 μg/mL and 80% with IMB dosage less than 100 μg/mL. Ep-IMB as well as Vi-IMB

 

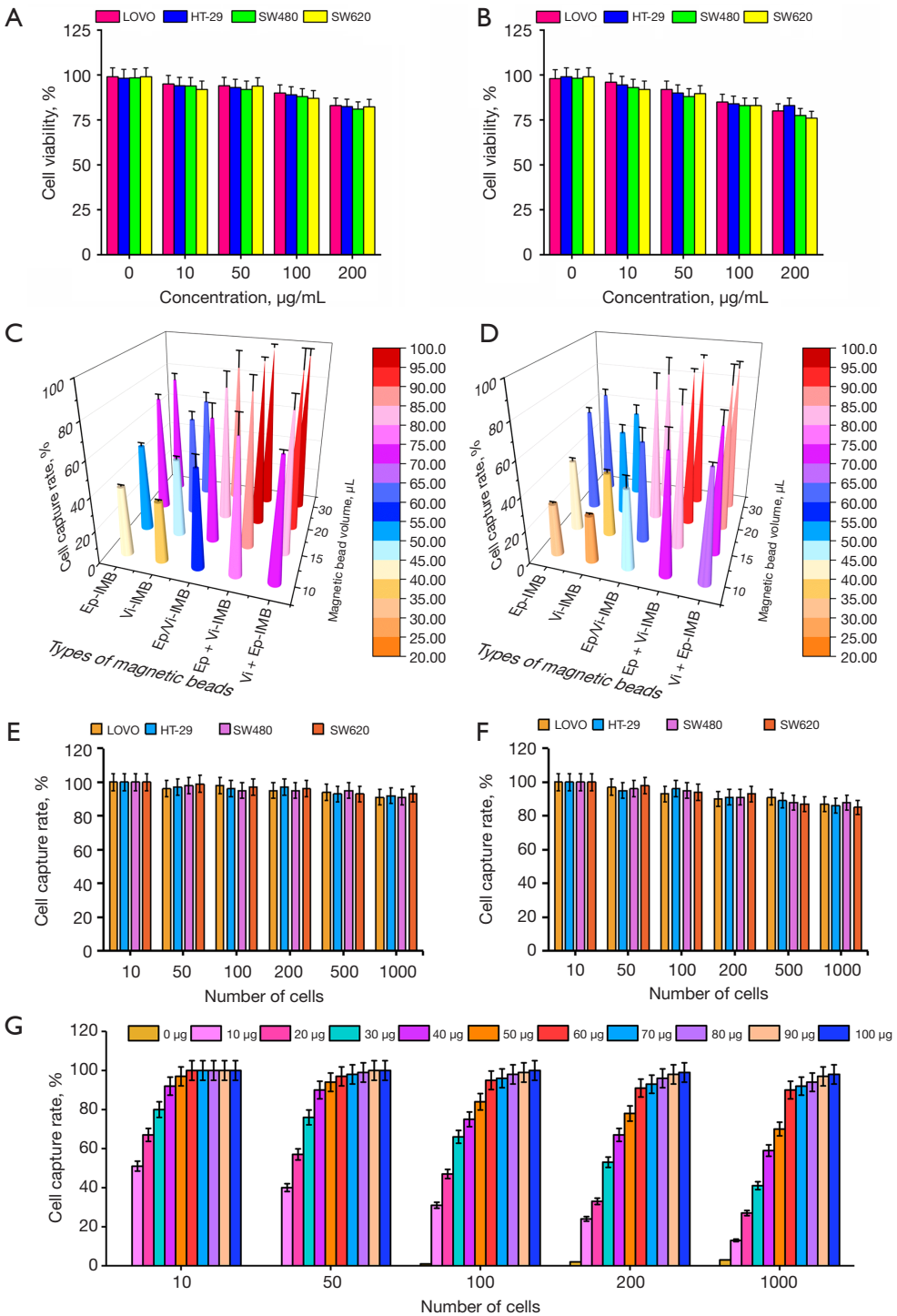


**Figure 2** Toxicity and capture efficiency testing of magnetic beads. (A) Toxicity assessment of Ep-IMB; (B) toxicity assessment of Vi-IMB; (C) capture efficiency of various IMB combination strategies in PBS environment; (D) capture efficiency of various magnetic bead combination strategies under analog blood environment; (E) validation of magnetic bead specificity in a PBS system; (F) validation of magnetic bead sensitivity in a blood simulation system; (G) evaluation of the capture efficiency of magnetic beads against antibody gradients. Ep-IMB, EpCAM-coated immunoliposomal magnetic beads; EpCAM, epithelial cell adhesion molecule; Vi-IMB, vimentin-coated immunoliposomal magnetic beads; Ep, Ep-IMB; Vi, Vi-IMB; PBS, phosphate buffer solution.

 

showed concentration-dependent cytotoxicity on tumor cells, and this trend was evident when the concentration of the IMBs was in the range of 50–200 μg/mL, indicating that the immunizing magnetic beads are toxic to cells when their concentration is too high. However, previous experiments have shown these magnetic beads to be relatively less toxic to tumor cells overall. Next, we further evaluated the capture efficiency of CRC cells under various IMB combination strategies by *in vitro* experiments as shown in *Figure 2C,2D*. The Ep-IMB + Vi-IMB group had the highest capture efficiency when the total number of beads was kept constant. We continued to evaluate the capture efficiency under the analog blood environment and found that the results were consistent with those that we tested in the PBS environment. We assessed the specificity of the combined application of Ep-IMB and Vi-IMB to capture CRC cell lines in the PBS environment to be 94.85% (*Figure 2E*), and the sensitivity of this capture strategy, for CRC cell lines, in the simulated blood environment to be 91.23% (*Figure 2F*). In order to further determine the optimal antibody dosage in the magnetic bead enrichment system, we evaluated gradient dose of antibody-coated magnetic beads to capture HT-29 cell lines and found that the optimal capture efficiency could be obtained when the antibody dose was adjusted to 60 μg (*Figure 2G*).

### *Participant characteristics*

Half of the participants were 69 years old or less; 61 were males and 49 were females. A total of 19 patients had lesions in the ascending colon (17.3%), 10 patients had lesions in the transverse colon (9.1%), 5 patients had tumors in the descending colon (4.5%), and 34 patients had tumors in the sigmoid colon (30.9%). A total of 25 patients had tumors in the cecum (22.7%), 9 patients had tumors in the hepatic curve (8.2%), 5 patients had tumors in the splenic curve (4.5%), and 3 patients had tumors in the rectum (2.7%). Of these patients, 3 (2.7%) were in stage I, 20 (18.2%) in stage II, 37 (33.6%) in stage III, and 50 (45.5%) in stage IV. The baseline characteristics of these patients are shown in *Table 1*.

### *Identification and counting of CTCs*

All cell suspensions enriched by magnetic beads were homogeneously spread on slides and sequentially added with CK-FITC, CD45-PE, and DAPI. Epithelial CTCs were defined as Ep-IMB-enriched tumor cells and $CK^+$/$CD45^-$/$DAPI^+$; mesenchymal CTCs were defined as Vi-IMB-enriched and $CK^+$/$CD45^-$/$DAPI^+$. We identified the number of CTCs in all participants and performed statistical analysis, as shown in *Figure 3A*. *Figure 3B* reveals that we found no significant difference in tumor cells enriched by Ep-IMB and Vi-IMB, however, the number of CTCs captured in the PB of healthy volunteers was significantly lower than that in patients with CRC (*Figure 3C,3D*). As shown in *Figure 3E-3G*, the areas under the curves (AUCs) for CRC diagnosis using total CTC, EP-IMB-enriched CTC, and Vi-IMB-enriched CTC were 0.872, 0.821, and 0.790, respectively. We found that total CTC exhibited the best diagnostic efficacy compared with the other two groups (*Figure 3E,3F*). We defined the threshold as five total CTCs per 7.5 mL of blood using Youden index (Figure S1).

### *Correlation between CTC enumeration and clinicopathologic*

In this study, a total of 110 patients with CRC and 25 healthy volunteers had their PB collected, and CTC and tumor marker analyses were performed separately. No clinicopathologic factors were found to be associated with the number of CTCs in PB. The correlations of CTC number with clinicopathologic parameters in CRC patients are shown in *Table 2*.

The median survival for the entire cohort was 29.9 months (95% CI: 17.9–29.9). The 1-, 3-, and 5-year survival rates were 93.6%, 89.1%, and 80.9%, respectively.

### *Predictors of survival*

We selected several candidate indicators that are clinically relevant to CRC patients from their baseline characteristics information: age, gender, tumor site, tumor morphology, AJCC stage, CTC number, CEA level (Table S1), and after incorporating the above information into the Cox regression model, we used the AIC to perform a backward stepwise selection strategy to identify the four variables that were the most relevant to the survival rate. Those four variables were identified as lymph node metastasis, AJCC stage, number of CTCs, and CEA level. Table S2 shows the hazard ratio (HR) and 95% CI of the multivariate Cox risk regression analysis optimized according to AIC. Total CTC count (HR, 1.09; 95% CI: 1.02–1.17) was an independent risk factor for poor prognosis, whereas AJCC stage, lymph node metastasis, and CEA level were associated with prognosis. We found that the highest risk of mortality was associated with the AJCC

 

**Table 1** Clinicopathologic features of patients with CRC

| Base line characteristics | Value |
|---|---|
| Gender | |
| Male | 61 (55.5) |
| Female | 49 (44.5) |
| Age (years) | 69 [61, 76] |
| Tumor location | |
| Cecum | 25 (22.7) |
| Ascending colon | 19 (17.3) |
| Descending colon | 5 (4.5) |
| Sigmoid colon | 34 (30.9) |
| Transverse colon | 10 (9.1) |
| Hepatic curve | 9 (8.2) |
| Splenic curve | 5 (4.5) |
| Rectum | 3 (2.7) |
| Metastasis location | |
| Arm, adrenal | 1 (0.9) |
| Bone | 1 (0.9) |
| Liver | 40 (36.4) |
| Lung, liver | 5 (4.5) |
| Breast, skin | 1 (0.9) |
| Pelvis, skin | 1 (0.9) |
| Spleen, liver | 1 (0.9) |
| Surgical resection | |
| R0 | 85 (77.3) |
| R1 | 25 (22.7) |
| *KRAS* mutant | |
| Wild type | 39 (35.5) |
| Mutant | 71 (64.5) |
| BRAF mutant | |
| Mutant | 5 (4.5) |
| Wild type | 105 (95.5) |
| Histologic typing | |
| Adenocarcinoma | 59 (53.6) |
| Adenocarcinoma intestinal type | 31 (28.2) |
| Mucinous adenocarcinoma | 19 (17.3) |
| Signet ring cell carcinoma | 1 (0.9) |
| AJCC stage | |
| I | 3 (2.7) |
| II | 20 (18.2) |
| III | 37 (33.6) |
| IV | 50 (45.5) |
| Neoadjuvant treated | |
| No | 110 (100.0) |
| Tumor stage | |
| I | 1 (0.9) |
| II | 5 (4.5) |
| III | 84 (76.4) |
| IV | 20 (18.2) |
| Nodes stage | |
| N0 | 33 (30.0) |
| N1 | 36 (32.7) |
| N2 | 41 (37.3) |
| Metastasis stage | |
| M0 | 78 (70.9) |
| M1 | 32 (29.1) |
| Total CTC (number) | 7.00 [5.00, 9.00] |
| CEA (ng/mL) | 4.20 [2.82, 5.70] |

Data are presented as n (%) or median [IQR]. CRC, colorectal cancer; AJCC, American Joint Committee on Cancer; CTC, circulating tumor cell; CEA, carcinoembryonic antigen; IQR, interquartile range.

stage of the tumor. We then created a nomogram based on the four variables screened by the model, and each variable was assigned a weighted score, which implies a prognosis; the lower the total score, the worse the prognosis. Based on the above variables, we plotted nomograms in which each variable was quantified, which means that the lower the score, the worse the survival prognosis. The nomogram for predicting 3-year survival in CRC patients is shown in *Figure 4*.

## Discussion

CRC deaths are the second highest in the world with

 

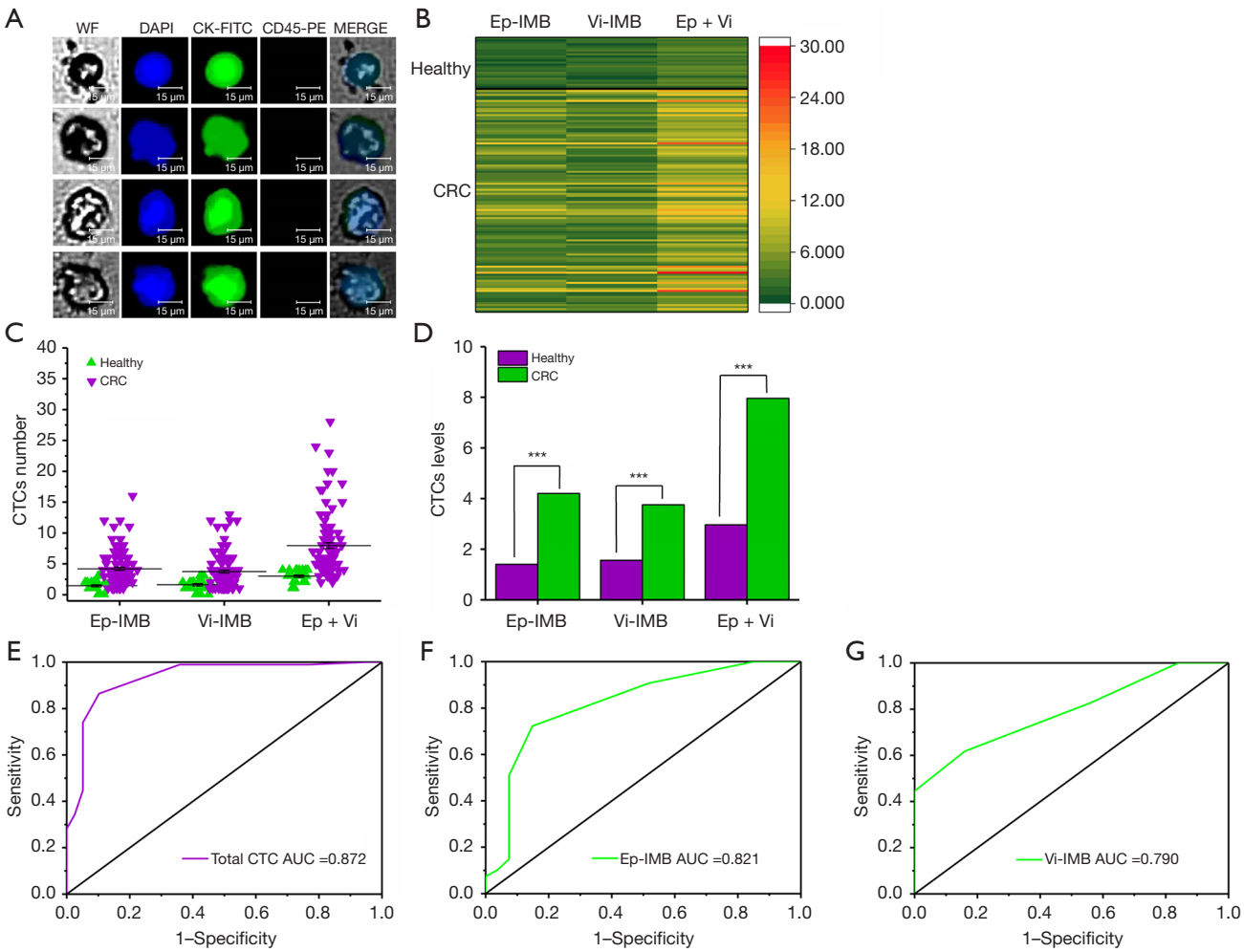


**Figure 3** CTC distribution in healthy volunteers and CRC patients. (A) Panel of typical CTC images from CRC patients; (B) distribution of CTCs enriched by different magnetic beads; (C) distribution of CTC number in healthy volunteers and CRC patients captured by Ep-IMB, Vi-IMB; (D) distribution of the difference in mean CTC levels between the healthy volunteers and CRC patients captured by combined Ep-IMB and Vi-IMB; (E) ROC curve of total CTC counts with 1 – specificity (= false positive rate) as X-axis and sensitivity as Y-axis to discriminate between CRC patients and healthy volunteers; (F) ROC curves of CTCs counted by EP-IMB distinguish CRC patients from healthy volunteers; (G) ROC curves of CTCs counted by Vi-IMB distinguish CRC patients from healthy volunteers. ***, indicates a significant difference (P<0.001). WF, wide field; DAPI, 4',6-diamidino-2-phenylindole; CRC, colorectal cancer; Ep-IMB, EpCAM-coated immunoliposomal magnetic beads; EpCAM, epithelial cell adhesion molecule; Vi-IMB, vimentin-coated immunoliposomal magnetic beads; Ep, Ep-IMB; Vi, Vi-IMB; CTC, circulating tumor cell; AUC, area under the curve; ROC, receiver operating characteristic.

approximately more than 1.8 million new cases and 881,000 deaths annually (23). Despite significant progress in CRC treatment in recent years, many tumors still recur and metastasize. Studies have shown that the 5-year survival rate of CRC patients is only 65%, and about half of CRC patients will eventually relapse and metastasize (24,25). CellSearch® enables clinical surveillance of patients with CRC (26-29), in addition there is a high association between the number of CTCs and clinical outcome in tumor patients (30). Since some of the CTCs lack EpCAM expression, they could not be analyzed using CellSearch®, which limited the Clinical practice of CTCs. We used non-EpCAM based CTC assays to improve the efficiency of CTC capture under EMT. It has been previously reported that a multi-target magnetic bead enrichment strategy has excellent capture efficiency compared to CellSearch® (31).

 

**Table 2** Correlation between the number of CTCs and clinicopathologic parameters

| Clinical pathological | <5 CTCs (n=23) | ≥5 CTCs (n=87) | P value |
|---|---|---|---|
| Gender | | | 0.976 |
| Female | 10 (43.5) | 39 (44.8) | |
| Male | 13 (56.5) | 48 (55.2) | |
| Age (years) | 67.00 (65.00, 75.50) | 69.00 (60.50, 76.00) | 0.506 |
| AJCC stage | | | 0.634 |
| I | 0 (0.0) | 3 (3.4) | |
| II | 3 (13.0) | 17 (19.5) | |
| III | 10 (43.5) | 27 (31.0) | |
| IV | 10 (43.5) | 40 (46.0) | |
| Tumor location | | | 0.314 |
| Cecum | 6 (26.1) | 19 (21.8) | |
| Ascending colon | 4 (17.4) | 15 (17.2) | |
| Descending colon | 1 (4.3) | 4 (4.6) | |
| Sigmoid colon | 7 (30.4) | 27 (31.0) | |
| Transverse colon | 0 (0.0) | 10 (11.5) | |
| Hepatic curve | 1 (4.3) | 8 (9.2) | |
| Splenic curve | 2 (8.7) | 3 (3.4) | |
| Rectum | 2 (8.7) | 1 (1.1) | |
| Metastasis location | | | 0.171 |
| Arm, adrenal | 1 (4.3) | 0 (0.0) | |
| Bone | 0 (0.0) | 1 (1.1) | |
| Liver | 6 (26.1) | 34 (39.1) | |
| Lung, liver | 2 (8.7) | 3 (3.4) | |
| Breast, skin | 1 (4.3) | 0 (0.0) | |
| Pelvis, skin | 0 (0.0) | 1 (1.1) | |
| Spleen, liver | 0 (0.0) | 1 (1.1) | |
| Surgical resection | | | 0.401 |
| R0 | 16 (69.6) | 69 (79.3) | |
| R1 | 7 (30.4) | 18 (20.7) | |
| *KRAS* mutant | | | 0.417 |
| Mutant | 6 (26.1) | 33 (37.9) | |
| Wild type | 17 (73.9) | 54 (62.1) | |
| *BRAF* mutant | | | >0.99 |
| Mutant | 1 (4.3) | 4 (4.6) | |
| Wild type | 22 (95.7) | 83 (95.4) | |

**Table 2** (*continued*)

 

**Table 2** (*continued*)

| Clinical pathological | <5 CTCs (n=23) | ≥5 CTCs (n=87) | P value |
|---|---|---|---|
| Histologic typing | | | 0.827 |
| Adenocarcinoma | 14 (60.9) | 45 (51.7) | |
| Adenocarcinoma intestinal type | 6 (26.1) | 25 (28.7) | |
| Mucinous adenocarcinoma | 3 (13.0) | 16 (18.4) | |
| Signet ring cell carcinoma | 0 (0.0) | 1 (1.1) | |
| Neoadjuvant treated | | | NA |
| No | 23 (100.0) | 87 (100.0) | |
| Tumor stage | | | 0.921 |
| I | 0 (0.0) | 1 (1.1) | |
| II | 1 (4.3) | 4 (4.6) | |
| III | 17 (73.9) | 67 (77.0) | |
| IV | 5 (21.7) | 15 (17.2) | |
| Nodes stage | | | 0.237 |
| N0 | 5 (21.7) | 28 (32.2) | |
| N1 | 11 (47.8) | 25 (28.7) | |
| N2 | 7 (30.4) | 34 (39.1) | |
| Metastasis stage | | | 0.679 |
| M0 | 18 (78.3) | 60 (69.0) | |
| M1 | 5 (21.7) | 27 (31.0) | |
| Total CTC (number) | 4.00 (3.00,4.00) | 8.00 (6.00,10.00) | <0.001 |
| CEA (ng/mL) | 2.80 (2.35,4.40) | 4.60 (3.15,6.05) | 0.008 |

Data are presented as n (%) or median (IQR). CTC, circulating tumor cell; AJCC, American Joint Committee on Cancer; NA, not available; CEA, carcinoembryonic antigen; IQR, interquartile range.

This is mainly due to the fact that we constructed Vi-IMB, which enhances the capture of vimentin-expressing CTC. Our study showed that the sensitivity of the assay system was 79% and the specificity was 100% when the cutoff was CTC was 5/7.5 mL of PB. This suggests that CTC has superior diagnostic efficacy for patients with CRC. Cao *et al.* used CTC to detect patients with gastric cancer with a sensitivity of 85% (32). Ntouroupi *et al.* applied CTC to detect CRC patients with 100% specificity and 92% sensitivity (33). We compared the performance of total CTC and CTCs enriched by EP-IMB/Vi-IMB, respectively, for the diagnosis of CRC and found that the diagnostic efficacy of total CTC was better than that of EP-IMB or Vi-IMB individually. We note that CTC was an independent prognostic factor in this paper, even though it did not correlate with any of the clinicopathologic parameters. We hypothesize that this phenomenon occurred because we included the total number of mixed epithelial CTCs and mesenchymal CTCs in our statistical calculations. CTCs are distinctly heterogeneous. Currently, it is possible to categorize CTCs into epithelial and mesenchymal types based on the antibodies expressed by the CTCs, and it has been found that these two types of CTCs are distinctly heterogeneous in the process of metastasis. The phenotypes of the two types of CTCs in the metastatic process are very different, and epithelial-type CTCs are associated with the formation of distal metastatic foci, whereas mesenchymal-type CTCs have a weaker ability to form metastatic foci, which is mainly related to the tumor's chemotherapy resistance (34). Therefore, when two types of CTCs with

 

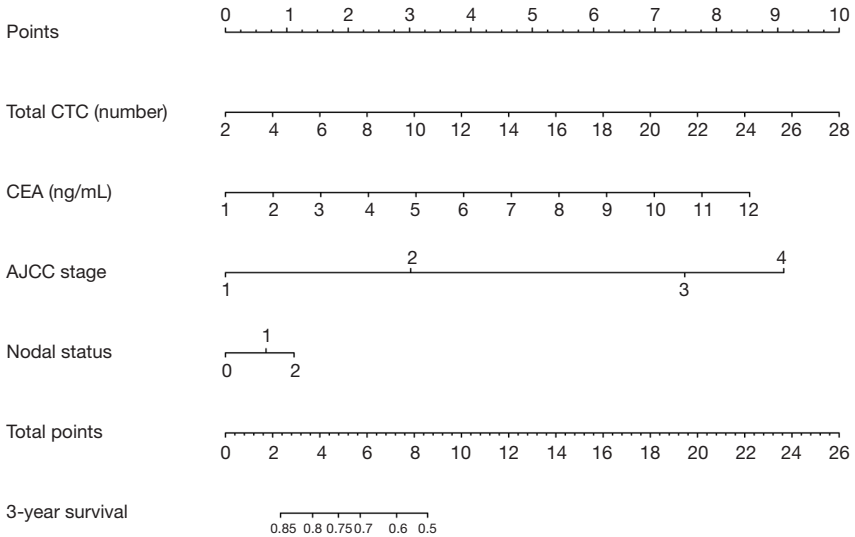


**Figure 4** Predicting 3-year survival in CRC patients with nomogram. CTC, circulating tumor cell; CEA, carcinoembryonic antigen; AJCC, American Joint Committee on Cancer; CRC, colorectal cancer.

different invasive abilities are mixed together, some features tend to be masked. However, both CTC subgroups are associated with poor patient prognosis, and we reanalyzed epithelial CTCs alone with the baseline characteristics of the cohort and found that CTCs were significantly associated with the pathological stage of AJCC in the cohort (Table S3). In addition, CTC also became an independent predictor of tumor prognosis (35); this contrasts with the work by Sotelo *et al.*, wherein CellSearch® was used to test 472 patients with stage III CRC, suggesting that CTC ≥1 is not a critical risk factor for OS (36). However, CTC quantities were associated with elevated tumor recurrence and worse prognosis (37), which our findings are consistent with. We used nomograms to demonstrate the long-term survival prognosis of CRC patients after surgery, which reflected that the number of CTCs, the level of CEA, the AJCC stage, and the status of lymph node metastasis adversely affected the survival. We can examine the effects of various clinical indicators on survival, and help clinicians better predict the patient outcomes and adopt personalized treatment measures to improve the survival status of patients. Our study also showed that a CTC classifier integrating non-invasive and reproducible features is more feasible and less costly than prognostic features in previous studies. Unlike traditional nomograms that use clinical prognostic factors, since CTC levels can reflect the malignancy of the primary tumor, we also incorporated CTC counts into a nomogram that predicts the survival risk of individual patients. Our statistical model demonstrated that elevated CTC counts were significantly associated with lower survival in patients with CRC, so incorporating CTC counts into this nomogram helped to improve its predictive accuracy. This will pave the way for the creation of a simple and accurate prognostic prediction method for CRC patients. As this is a retrospective study, the prediction of survival outcomes may have been affected by the short follow-up period and the small number of observed cases. We will further expand the sample size and extend the follow-up time to more comprehensively evaluate the prognostic value of CTC in the assessment of CRC patients.

## Conclusions

CTCs can be recognized as a novel biomarker that can provide valuable information for screening people at high risk of CRC. Our study also demonstrated that CTC is an independent prognostic indicator for OS, nomograms can evaluate the effect of multiple variables on the probability of long-term survival in individual patients (38,39). In the future, we will further expand the sample size and follow-up time to improve the prognostic research of CTC.

## Acknowledgments

*Funding:* This study was supported by the Health

 

Development Promotion Project (No. KM-JSQY-006).

## Footnote

*Reporting Checklist:* The authors have completed the TRIPOD reporting checklist. Available at https://jgo.amegroups.com/article/view/10.21037/jgo-23-735/rc

*Data Sharing Statement:* Available at https://jgo.amegroups.com/article/view/10.21037/jgo-23-735/dss

*Peer Review File:* Available at https://jgo.amegroups.com/article/view/10.21037/jgo-23-735/prf

*Conflicts of Interest:* All authors have completed the ICMJE uniform disclosure form (available at https://jgo.amegroups.com/article/view/10.21037/jgo-23-735/coif). The authors have no conflicts of interest to declare.

*Ethical Statement:* The authors are accountable for all aspects of the work in ensuring that questions related to the accuracy or integrity of any part of the work are appropriately investigated and resolved. The study was conducted in accordance with the Declaration of Helsinki (as revised in 2013) and was approved by the Ethics Committee of Huadong Hospital Affiliated to Fudan University (No. 20230056). Written informed consent has been signed from patients before participation.



## References

1. World Cancer Research Fund International. [Cited 2023 Jul 1]. Available from: https://www.wcrf.org/
2. Morgan E, Arnold M, Gini A, et al. Global burden of colorectal cancer in 2020 and 2040: incidence and mortality estimates from GLOBOCAN. Gut 2023;72:338-44.
3. Janczewski LM, Faski J, Nelson H, et al. Survival outcomes used to generate version 9 American Joint Committee on Cancer staging system for anal cancer. CA Cancer J Clin 2023;73:516-23.
4. Kryza D, Wischhusen J, Richaud M, et al. From netrin-1-targeted SPECT/CT to internal radiotherapy for management of advanced solid tumors. EMBO Mol Med 2023;15:e16732.
5. Baptistella AR, Salles Dias MV, Aguiar S Jr, et al. Heterogeneous expression of A33 in colorectal cancer: possible explanation for A33 antibody treatment failure. Anticancer Drugs 2016;27:734-7.
6. Cheal SM, Fung EK, Patel M, et al. Curative Multicycle Radioimmunotherapy Monitored by Quantitative SPECT/CT-Based Theranostics, Using Bispecific Antibody Pretargeting Strategy in Colorectal Cancer. J Nucl Med 2017;58:1735-42.
7. Yoshino T, Cervantes A, Bando H, et al. Pan-Asian adapted ESMO Clinical Practice Guidelines for the diagnosis, treatment and follow-up of patients with metastatic colorectal cancer. ESMO Open 2023;8:101558.
8. Pereira-Veiga T, Schneegans S, Pantel K, et al. Circulating tumor cell-blood cell crosstalk: Biology and clinical relevance. Cell Rep 2022;40:111298.
9. Kapeleris J, Ebrahimi Warkiani M, Kulasinghe A, et al. Clinical Applications of Circulating Tumour Cells and Circulating Tumour DNA in Non-Small Cell Lung Cancer-An Update. Front Oncol 2022;12:859152.
10. Bankó P, Lee SY, Nagygyörgy V, et al. Technologies for circulating tumor cell separation from whole blood. J Hematol Oncol 2019;12:48.
11. Yeo D, Kao S, Gupta R, et al. Accurate isolation and detection of circulating tumor cells using enrichment-free multiparametric high resolution imaging. Front Oncol 2023;13:1141228.
12. O'Leary K. Nocturnal habits of circulating tumor cells. Nat Med 2022. [Epub ahead of print]. doi: 10.1038/d41591-022-00075-3.
13. Cieślikowski WA, Milecki P, Świerczewska M, et al. Baseline CTC Count as a Predictor of Long-Term Outcomes in High-Risk Prostate Cancer. J Pers Med 2023;13:608.
14. Chen L, Zhou W, Ye Z, et al. Predictive Value of Circulating Tumor Cells Based on Subtraction Enrichment for Recurrence Risk in Stage II Colorectal Cancer. ACS Appl Mater Interfaces 2022;14:35389-99.
15. Vidlarova M, Rehulkova A, Stejskal P, et al. Recent Advances in Methods for Circulating Tumor Cell Detection. Int J Mol Sci 2023;24:3902.

 

16. Gabriel MT, Calleja LR, Chalopin A, et al. Circulating Tumor Cells: A Review of Non-EpCAM-Based Approaches for Cell Enrichment and Isolation. Clin Chem 2016;62:571-81.
17. Lawrence R, Watters M, Davies CR, et al. Circulating tumour cells for early detection of clinically relevant cancer. Nat Rev Clin Oncol 2023;20:487-500.
18. Kitz J, Goodale D, Postenka C, et al. EMT-independent detection of circulating tumor cells in human blood samples and pre-clinical mouse models of metastasis. Clin Exp Metastasis 2021;38:97-108.
19. Ju S, Chen C, Zhang J, et al. Detection of circulating tumor cells: opportunities and challenges. Biomark Res 2022;10:58.
20. Poudineh M, Aldridge PM, Ahmed S, et al. Tracking the dynamics of circulating tumour cell phenotypes using nanoparticle-mediated magnetic ranking. Nat Nanotechnol 2017;12:274-81.
21. Zhang X, Xie P, Zhang K, et al. Circulating tumour cell isolation, analysis and clinical application. Cell Oncol (Dordr) 2023;46:533-44.
22. Huang C, Ding S, Huang C, et al. Distribution and Clinical Analysis of EpCAM+/Vimentin+ Circulating Tumor Cells in High-Risk Population and Cancer Patients. Front Oncol 2021;11:642971.
23. Jenkins R, Walker J, Roy UB. 2022 cancer statistics: Focus on lung cancer. Future Oncol 2023. [Epub ahead of print]. doi: 10.2217/fon-2022-1214.
24. Miller KD, Nogueira L, Devasia T, et al. Cancer treatment and survivorship statistics, 2022. CA Cancer J Clin 2022;72:409-36.
25. Lambert AW, Pattabiraman DR, Weinberg RA. Emerging Biological Principles of Metastasis. Cell 2017;168:670-91.
26. Vasantharajan SS, Barnett E, Gray ES, et al. Assessment of a Size-Based Method for Enriching Circulating Tumour Cells in Colorectal Cancer. Cancers (Basel) 2022;14:3446.
27. Nomura M, Yokoyama Y, Yoshimura D, et al. Simple Detection and Culture of Circulating Tumor Cells from Colorectal Cancer Patients Using Poly(2-Methoxyethyl Acrylate)-Coated Plates. Int J Mol Sci 2023;24:3949.
28. Sisodiya S, Kasherwal V, Khan A, et al. Liquid Biopsies: Emerging role and clinical applications in solid tumours. Transl Oncol 2023;35:101716.
29. Orrapin S, Thongkumkoon P, Udomruk S, et al. Deciphering the Biology of Circulating Tumor Cells through Single-Cell RNA Sequencing: Implications for Precision Medicine in Cancer. Int J Mol Sci 2023;24:12337.
30. Slovin SF, Knudsen K, Halabi S, et al. Randomized Phase II Multicenter Trial of Abiraterone Acetate With or Without Cabazitaxel in the Treatment of Metastatic Castration-Resistant Prostate Cancer. J Clin Oncol 2023;41:5015-24.
31. Lu X, Tan S, Wu M, et al. Evaluation of a new magnetic bead as an integrated platform for systematic CTC recognition, capture and clinical analysis. Colloids Surf B Biointerfaces 2021;199:111542.
32. Cao B, Liu L, Zhang R, et al. Sensitivity and specificity of folate receptor α-positive circulating tumour cells in gastric cancer. Postgrad Med J 2024;100:112-9.
33. Ntouroupi TG, Ashraf SQ, McGregor SB, et al. Detection of circulating tumour cells in peripheral blood with an automated scanning fluorescence microscope. Br J Cancer 2008;99:789-95.
34. Liu X, Li J, Cadilha BL, et al. Epithelial-type systemic breast carcinoma cells with a restricted mesenchymal transition are a major source of metastasis. Sci Adv 2019;5:eaav4275.
35. Thery L, Meddis A, Cabel L, et al. Circulating Tumor Cells in Early Breast Cancer. JNCI Cancer Spectr 2019;3:pkz026.
36. Sotelo MJ, Sastre J, Maestro ML, et al. Role of circulating tumor cells as prognostic marker in resected stage III colorectal cancer. Ann Oncol 2015;26:535-41.
37. Pan RJ, Hong HJ, Sun J, et al. Detection and Clinical Value of Circulating Tumor Cells as an Assisted Prognostic Marker in Colorectal Cancer Patients. Cancer Manag Res 2021;13:4567-78.
38. Pulvirenti A, Javed AA, Landoni L, et al. Multi-institutional Development and External Validation of a Nomogram to Predict Recurrence After Curative Resection of Pancreatic Neuroendocrine Tumors. Ann Surg 2021;274:1051-7.
39. Levy DA, Li H, Sterba KR, et al. Development and Validation of Nomograms for Predicting Delayed Postoperative Radiotherapy Initiation in Head and Neck Squamous Cell Carcinoma. JAMA Otolaryngol Head Neck Surg 2020;146:455-64.

**Cite this article as:** Wang Y, Xia L, Wu M, Huang C. Prognostic evaluation of a multi-target magnetic bead-enriched circulating tumor cell-enriched identification system for colorectal cancer. J Gastrointest Oncol 2024;15(1):134-146. doi: 10.21037/jgo-23-735

 

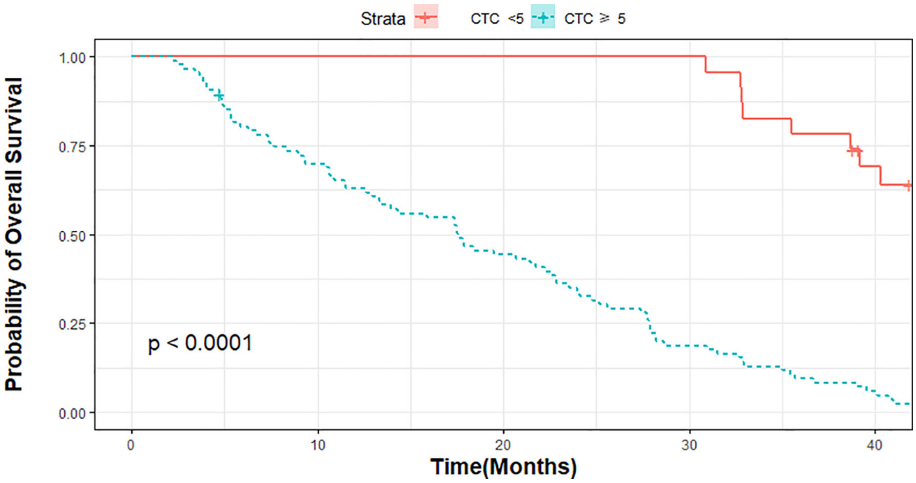


**Figure S1** Kaplan-Meier curve for OS based on total CTC counts. CTC, circulating tumor cell; OS, overall survival.


https://dx.doi.org/10.21037/jgo-23-735

**Tables S1** Univariate analysis of Cox proportional hazards regression model

| Variables | Univariate model, HR (95% CI) | P value |
|---|---|---|
| Gender | | |
| Female | 1.00 (Reference) | 0.5 |
| Male | 0.86 (0.58–1.29) | |
| Tumor location | | |
| Cecum | 1.00 (Reference) | 0.5 |
| Ascending colon | 0.94 (0.50–1.78) | |
| Descending colon | 1.38 (0.54–3.49) | |
| Sigmoid colon | 0.61 (0.34–1.09) | |
| Transverse colon | 0.73 (0.33–1.63) | |
| Hepatic curve | 0.57 (0.23–1.43) | |
| Splenic curve | 0.90 (0.33–2.41) | |
| Rectum | 0.67 (0.23–2.00) | |
| Tumor morphology | | |
| Adenocarcinoma | 1.00 (Reference) | 0.4 |
| Adenocarcinoma intestinal type | 1.25 (0.76–2.03) | |
| Mucinous adenocarcinoma | 1.34 (0.77–2.32) | |
| Signet ring cell carcinoma | 0.32 (0.04–2.35) | |
| AJCC stage | | |
| I | 1.00 (Reference) | 0.004 |
| II | 1.02 (0.11–8.52) | |
| III | 4.71 (0.65–34.14) | |
| IV | 5.82 (0.78–43.69) | |
| CEA (≥5 *vs.* <5 ng/mL) | 3.77 (2.43–5.84) | <0.001 |
| Nodal status | | |
| N0 | 1.00 (Reference) | 0.09 |
| N1 | 1.39 (0.84–2.31) | |
| N2 | 1.69 (1.05–2.71) | 0.03 |
| Age (≥70 *vs.* <70 years) | 1.34 (0.90–1.99) | 0.2 |
| Total CTC (≥5 *vs.* <5) | 8.41 (4.22–16.75) | <0.001 |

HR, hazard ratio; CI, confidence interval; AJCC, American Joint Committee on Cancer; CEA, carcinoembryonic antigen; CTC, circulating tumor cell.


https://dx.doi.org/10.21037/jgo-23-735

**Table S2** Multivariate analysis of Cox proportional hazards regression model

| Variables | Multivariate model, HR (95% CI) | P value |
|---|---|---|
| Nodal status | | |
| N0 | 1 (Reference) | |
| N1 | 1.17 (0.68–1.99) | 0.08 |
| N2 | 1.30 (0.79–2.13) | 0.05 |
| AJCC stage | | |
| I | 1.00 (Reference) | |
| II | 2.02 (0.22–18.89) | 0.54 |
| III | 5.71 (0.78–41.95) | 0.09 |
| IV | 8.31 (1.09–63.20) | 0.04 |
| Total CTC (number) | 1.09 (1.02–1.17) | 0.01 |
| CEA (ng/mL) | 1.20 (1.00–1.44) | 0.05 |

HR, hazard ratio; CI, confidence interval; AJCC, American Joint Committee on Cancer; CTC, circulating tumor cell; CEA, carcinoembryonic antigen.


https://dx.doi.org/10.21037/jgo-23-735

**Table S3** Correlation between the number of CTCs enriched by Ep-IMB and clinicopathologic parameters

| Clinical pathological | <5 CTCs (n=51) | ≥5 CTCs (n=59) | P value |
|---|---|---|---|
| Gender | | | 0.764 |
| Female | 24 (47.1) | 25 (42.4) | |
| Male | 27 (52.9) | 34 (57.6) | |
| Age (years) | 71.00 (63.50, 75.50) | 68.00 (58.50, 76.00) | 0.263 |
| AJCC stage | | | <0.001 |
| I | 3 (5.9) | 0 (0.0) | |
| II | 18 (35.3) | 2 (3.4) | |
| III | 18 (35.3) | 19 (32.2) | |
| IV | 12 (23.5) | 38 (64.4) | |
| Tumor location | | | 0.078 |
| Cecum | 13 (25.5) | 12 (20.3) | |
| Ascending colon | 5 (9.8) | 14 (23.7) | |
| Descending colon | 4 (7.8) | 1 (1.7) | |
| Sigmoid colon | 18 (35.3) | 16 (27.1) | |
| Transverse colon | 1 (2.0) | 9 (15.3) | |
| Hepatic curve | 5 (9.8) | 4 (6.8) | |
| Splenic curve | 3 (5.9) | 2 (3.4) | |
| Rectum | 2 (3.9) | 1 (1.7) | |
| Histologic typing | | | 0.697 |
| Adenocarcinoma | 28 (54.9) | 31 (52.5) | |
| Adenocarcinoma intestinal type | 13 (25.5) | 18 (30.5) | |
| Mucinous adenocarcinoma | 10 (19.6) | 9 (15.3) | |
| Signet ring cell carcinoma | 0 (0.0) | 1 (1.7) | |

Data are presented as n (%) or median (IQR). CTC, circulating tumor cell; Ep-IMB, EpCAM-coated immunoliposomal magnetic beads; EpCAM, epithelial cell adhesion molecule; AJCC, American Joint Committee on Cancer; IQR, interquartile range.


https://dx.doi.org/10.21037/jgo-23-735